



PLEA 2017 EDINBURGH

Design to Thrive

Indoor comfort evaluation by natural ventilation in hot climates: Heat Balance Index

José Antonio Castillo¹ and Guadalupe Huelsz²

¹ Centro de Investigaciones en Arquitectura, Urbanismo y Paisaje, Facultad de Arquitectura, Universidad Nacional Autónoma de México, Ciudad Universitaria, Av. Universidad 3000, Coyoacán, 04510, Ciudad de México, México. Email: jacat@ier.unam.mx

² Instituto de Energías Renovables, Universidad Nacional Autónoma de México, A.P. 34 Temixco Centro, 62580, Temixco, Mor., México. Email: ghl@ier.unam.mx

Abstract: Natural ventilation is a passive alternative to create comfort and healthy indoor conditions. Particularly in hot humid climates, full day ventilation is the best strategy to promote thermal comfort conditions, because the increase of the airflow velocity increases the sweat evaporative cooling of the occupants. Thus, it is important to assess the indoor natural ventilation in terms of the thermal comfort. This work uses a novel method, the Heat Balance Index (HBI) to evaluate the thermal comfort of the occupants in terms of the indoor natural ventilation in hot climates. HBI gives a method to define the comfort velocity range useful to calculate the well-ventilated percentage of a space. HBI considers the metabolic heat production and the heat transfer between the body and the surrounding given by the mechanisms of radiation, convection and evaporation. The HBI is applied to a study case based on Computational Fluid Dynamics simulations of a room with a window and a windexchanger in one climate condition of a Mexican city. The study case simulations are validated with experiment results. The application example gives the percentages of the living volume with discomfort by low ventilation, with comfort by adequate ventilation and discomfort by high ventilation.

Keywords: Natural ventilation, hygrothermal comfort evaluation, CFD simulations, heat balance, hot-humid climate

Introduction

Natural ventilation is an alternative to provide comfort and healthy indoor conditions, reducing the energy consumption. Typically, the energy cost of a naturally ventilated building is 40% less than that of an air-conditioned building (EEBPP, 1993). For hot humid climates, full day ventilation is the better strategy to promote thermal comfort conditions (Liping and Hien, 2007), because the increase of the airflow velocity increases the sweat evaporative cooling of the occupants.

For ventilation performance evaluation, the most used parameters are the mean magnitude velocity at the space, U , and the concept of well-ventilated percentage of a space, P , that is defined by Bastide et al. (2006) as the percentage of the volume with velocities within a velocity range (U_{min} ; U_{max}). They show that the results are very sensitive to the choice of U_{min} and U_{max} , but they do not give a methodology to select these values.

For the evaluation of thermal comfort, the most common method is the Predicted Mean Vote, PMV, with the Predicted Percentage Dissatisfied, PPD, (Fanger, 1970). This method has been developed in controlled conditions, not in natural ventilated buildings.

However, the temperature ranges of validity of the models used by all these indices do not cover the high temperatures of hot climates. There are thermal comfort models useful for non air-conditioned spaces, i.e. naturally ventilated spaces, such as adaptive comfort temperature models that are functions of the monthly mean of the outdoor air temperature (De Dear and Brager, 2002; Humphreys and Nicol, 2000; Yang, 2003). Only one study was found that proposes a method for the evaluation of natural ventilation in terms of thermal comfort (Su et al., 2009). The authors propose temperature neutrality formulas, one for indoor air temperature over 28 °C and other for indoor air temperature below 28 °C, that are functions of the monthly mean of outdoor air temperature, the relative humidity and the airflow velocity near occupants. They considered a comfort zone band width of 4 °C. Unfortunately, the authors do not give details of the methodology followed to derive these formulas.

The Heat Stress Index, HSI, is a method used to evaluate thermal comfort for indoor in hot conditions (Belding and Hatch, 1955). It is defined as the ratio of the required evaporation to the maximum evaporative capacity of the air. The Index of Thermal Stress is a method to evaluate thermal comfort for outdoors in hot climates, ITS (Givoni 1969). Also for outdoors, but for cold climates, is the windchill correction (Aynsley, 1974).

The Heat Balance Index, HBI, (Castillo and Huelsz, 2017) provides a method to define the comfort velocity range ($U_{min}; U_{max}$) in hot climates. The HBI is useful to calculate the well-ventilated percentage of a space. In the next section, more details of HBI are given. This paper presents an application example of the HBI to evaluate the indoor natural ventilation in hot climates in terms of the thermal comfort of the occupants. The application example is applied in a room with a window and one windexchanger by using Computational Fluid Dynamics (CFD) simulations with one weather condition of a Mexican city.

Heat Balance Index

The thermal comfort is obtained when the metabolic heat production is totally transferred to the surroundings without heat stress, the Heat Balance Index, HBI, explained here, is defined as the ratio between the comfortable heat balance of the body and the metabolic heat production (Castillo and Huelsz, 2017). The comfortable heat balance of the body is given by the algebraic sum of the metabolic heat production and the heat transfer between the body and the surrounding given by the mechanisms of radiation, convection and evaporation,

$$HBI = \frac{M - R - C - E}{M} \quad (1)$$

where M , R , C and E are the metabolic heat production, and the heat transfer by radiation, convection and evaporation, respectively, all expressed in (W/m^2). The following empirical expressions for R , C and E (Wang et al., 2011) are used,

$$R = C_1 (T_s - T_r) \quad (2)$$

$$C = C_2 U^{3/5} (T_s - T_a) \quad (3)$$

$$E = C_3 U^{3/5} (P_s - P_a) \quad (4)$$

where $T_s = 35$ °C is the skin temperature, T_r (°C) is the mean radiant temperature, T_a (°C) is the ambient temperature, U (m/s) is the air velocity, P_a (10^2 Pa) is the partial pressure of water vapor and $P_s = 56 \times 10^2$ Pa is the vapor saturation pressure at T_s . The model constants

are $C_1 = 4.4 \text{ W/m}^2\text{°C}$ and $C_2 = 4.6 \text{ Ws}^{3/5}/\text{m}^{13/5}\text{°C}$. The factor C_3 for maximum evaporative capacity in Belding and Hatch (1955) has a constant value. In this work, the factor C_3 was modified for comfort evaporation by correlating results from the PMV comfort range (± 0.5), resulting in $C_3 = 26.903 - 0.857T_a - 0.003RH$; RH where is the relative humidity. When the value of C_3 is less than zero, it is considered as zero. These expressions are based on the assumptions that all the latent heat of sweat evaporation is drawn from the body and the skin temperature, $T_s = 35 \text{ °C}$, is constant. As the evaporation is only possible if $P_s > P_a$, if this condition is not fulfilled $E = 0$ in Eq. (4). Also, if the calculated value of $E < 0$, it is considered as zero. In this model the heat transfer by breathing is not considered. The heat transfer by this mechanism can represent up to 5% of the metabolic level considered in the present study (standing, light activity) and will represent a lower proportion for higher metabolic levels. As HBI is developed for hot climates, in the PMV calculation single layers of light weight clothing are considered, $I_{CL} = 0.05 \text{ m}^2\text{°C/W} = 0.32\text{Clo}$.

In Table 1, the range of conditions covered by the empirical expressions (Eq. (2) - (4)) used for the calculation of HBI are shown. These range of conditions, based on Wang et al. (2011), allow a proper application in hot climates, as the climate studied in this paper.

Table 1. The range of conditions covered by the HBI, based on Wang et al. (2011).

Lower limit		Upper limit
65 W/m ²	$\leq M \leq$	327 W/m ²
21 °C	$\leq T_a \leq$	31 °C
0.25 m/s	$\leq U \leq$	10.00 m/s
0 %	$\leq RH \leq$	100 %
$3 \times 10^2 \text{ Pa}$	$\leq P_a \leq$	$56 \times 10^2 \text{ Pa}$

A zero value of HBI represents the neutral thermal condition, where the heat generated by the body (M) is exactly equal to the heat transferred to the surroundings with comfort evaporation. For this work, the range $0.2 \leq \text{HBI} \leq 0.2$ is considered the comfort range. This range is obtained by correlating the PMV comfort range ($0.5 \leq \text{PMV} \leq 0.5$) with the HBI. $\text{HBI} < 0.2$ indicates that the body has an overdissipation greater than the 20%, with respect of M , causing a cold uncomfot. On the other hand, $\text{HBI} > 0.2$ signifies that the body has a subdissipation greater than the 20%, thus the body feels a hot uncomfot.

In order to evaluate the range for thermal comfort of the magnitude of the air velocity produced by natural ventilation, U is solved from Eq. (1) to Eq. (4),

$$U = \left[\frac{M(1 - \text{HBI}) - R}{C_2(T_s - T_a) + C_3(P_s - P_a)} \right]^{5/3} \quad (5)$$

As can be observed, U depends on HBI. Three magnitudes of U are distinguished: U_{min} , U_{neu} and U_{max} , for the HBI values of 0.2, 0.0 and 0.2, respectively. Thus $U_{min} \leq U \leq U_{max}$, represents the comfort air velocity range for a given activity (M value) and climatic conditions.

Windexchanger reference case

The windexchanger (WE) reference case has square-cross-section, one duct, four openings and flat roof. It is located on the center of a room roof. The WE has a height of 1.40 m measured from the roof, have a square-cross-section of 0.65 m in length and it is designed with a roof eave of 0.64 m as solar and rain protection. The interior dimensions of the room are $W \times D \times H = 3.0 \times 3.0 \times 2.7\text{m}^3$ (Fig. 1). The room has a square window at windward, 1.30 m

in length, giving a wall porosity (opening area divided by wall area) of 17% (Etheridge, 2012), it is centered on the wall and its base is at a height of 0.90 m from the floor.

Experiments

The room with the WE reference case was experimentally tested by (Cruz-Salas et al., 2014) using a scaled model (1:25), as shown in Fig. 1. The scaled model was set in the test section of an open water channel (OWC) and Stereo Particle Image Velocimetry (SPIV) measurements were carried out. The OWC is 6 m long and has a test section of $1.0 \times 0.315 \times 0.41 \text{ m}^3$. The scaled model is made of transparent acrylic, with thicknesses of 6 mm for walls and room's roof, 9 mm for the floor, and 3 mm for the WE roof. The interior dimensions are $W \times D \times H = 12 \times 12 \times 10.8 \text{ cm}^3$. The SPIV measurements were performed in the vertical central plane, as shown in Fig. 1b. In the OWC, an atmospheric boundary layer (open-terrain roughness profile) of a suburban area was reproduced. The mean velocity, U , and turbulence intensity, I , profiles were measured in the empty test section at the model position but without it, i.e. incident profiles. The obtained friction coefficient of the exponential law is $\alpha=0.29$ and the aerodynamic roughness length z_0 is 0.06 cm (for full scale, 0.015 m). The incident profiles are used for a reliable validation study as recommended by (Blocken et al., 2008). A reference mean wind speed $U_{ref} = 0.089 \text{ m/s}$ (for full scale, 0.062 m/s) and a reference turbulence intensity of 20% were measured at the reference height z_{ref} taken as the external height of the room $h = 12.3 \text{ cm}$ (for full scale, 3.075 m). The experiments were made in water applying the dynamic similarity with the Reynolds number $Re = U_{ref} z_{ref} / \nu = 1.23 \times 10^4$, where $\nu = 8.94 \times 10^{-7} \text{ m}^2/\text{s}$ is the kinematic viscosity at the water temperature $T_w = 25 \text{ }^\circ\text{C}$.

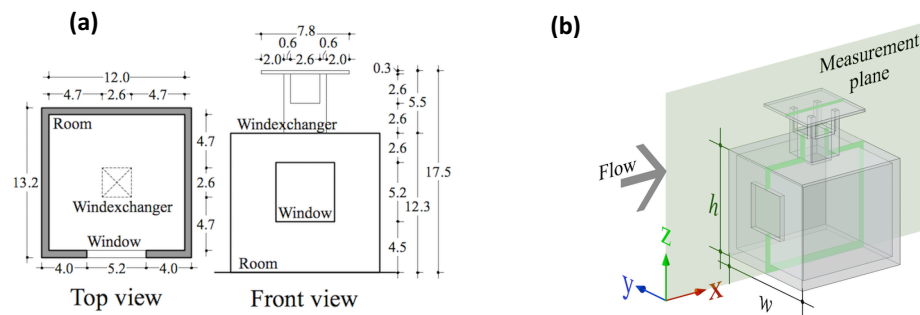


Figure 1. Model of the room with the windexchanger reference case. (a) Top and front view, units in centimeters; (b) Isometric view with the measurement plane and flow direction, where $h = 0.123 \text{ m}$ and $w = 0.132 \text{ m}$ are the external height and width of the room model, respectively.

CFD Validation

The present paper reports a CFD study performed with the commercial code COMSOL 5.1 (COMSOL 2013). This section presents the simulation model and settings for the validation of the room with the WE reference case. The settings are taken from a previous validation work (Castillo et al., 2014) using the experiments reported by (Cruz-Salas et al., 2014) and succinctly presented in previous section.

Model and settings

For the CFD simulations, the 3D steady RANS equations in combination with the shear-stress transport (SST) $k-\omega$ model are solved. The GMRES solver with MULTIGRID-SOR preconditioner is employed for velocity-pressure coupling, and the MULTIGRID-SCGS preconditioner is used

for viscous terms of the governing equations (COMSOL 2013). The convergence criteria is assumed to be obtained when all the scaled residuals are equal or less than 10^{-4} .

Computational domain and grid

The computational domain with the room with the WE reference case is developed following the best guidelines by (Tominaga et al. 2008; Ramponi and Blocken 2012), its dimensions are $W_d \times L_d \times H_d = 0.315 \times 2.346 \times 0.41 \text{ m}^3$ (Figure 2a). A tetrahedral grid is created with 1,176,225 nodes (Figure 2b).

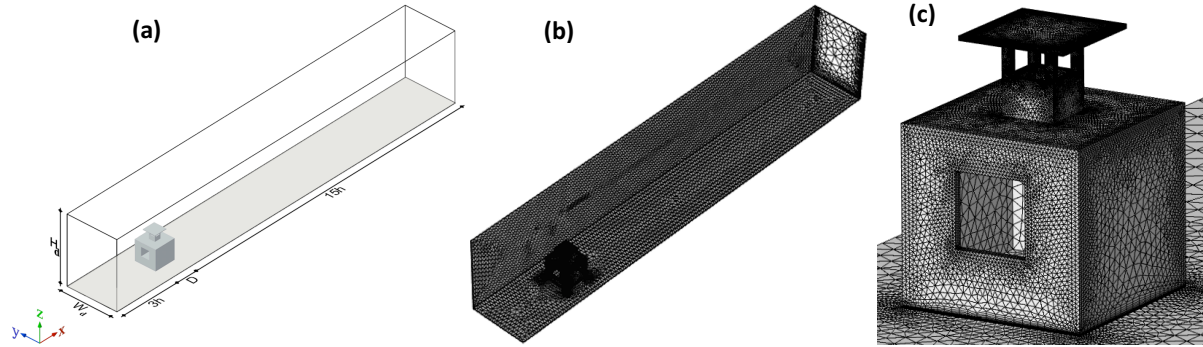


Figure 2. Computational domain with the model of the room with the WE reference case: (a) Perspective view with dimensions of the domain; (b) Perspective view of grid at bottom face (grid A with 1,176,225 nodes); (c) Isometric view of the room with the WE reference case.

Boundary conditions

The inlet boundary conditions are set according to the experimental velocity and turbulent profiles. The velocity profile is defined by the logarithmic law, $U(z) = (u^*_{ABL}/\kappa) \ln((z+z_0)/z_0)$, with the atmospheric boundary layer (ABL) friction velocity, $u^*_{ABL} = 0.007 \text{ m/s}$, the von Karman constant, $\kappa = 0.42$, the roughness length, $z_0 = 0.0005 \text{ m}$, and the height coordinate, z . The turbulent kinetic energy profile, $k(z) = (\sigma_u^2(z) + \sigma_v^2(z) + \sigma_w^2(z))/2$, is calculated from the standard deviation of each velocity component for x-direction, σ_u , for y-direction, σ_v , and for z-direction, σ_w . The turbulence dissipation rate and specific dissipation rate profiles are obtained, $\varepsilon(z) = u^{*3}_{ABL} / \kappa(z + z_0)$ and $\omega(z) = \varepsilon(z) / C_\mu k(z)$, respectively, with the empirical constant $C_\mu = 0.09$ (Tominaga et al. 2008). The standard wall functions (COMSOL 2013) are set at ground surface and at lateral walls. The zero static pressure is applied on the rear face of the domain. The free slip condition at the top boundary is used to simulate the air-water interface. In Fig. 3, the velocity profile and turbulent profiles, $k(z)$ and $\omega(z)$ at the inlet and incident building position in the empty domain are presented, showing that their streamwise gradients are negligible.

Validation

In Fig. 4, the experimental and CFD velocity vector fields at the central plane are shown, as well as the streamwise speed ratio, u/U_{ref} , along a horizontal line, L_h . The CFD simulation results show good agreement with the SPIV experimental results. The averaged difference of stream-wise speed ratios is lower than 10%.

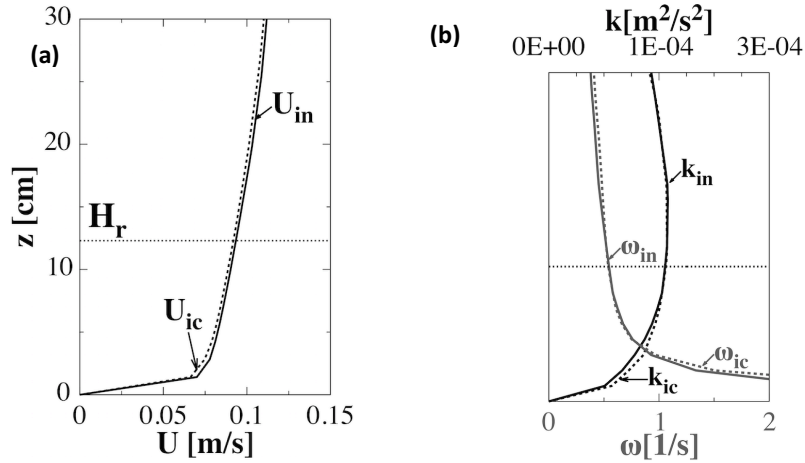


Figure 3. Vertical profiles of (left) the mean velocity, U ; (right) the turbulent kinetic energy (dark line), k , and the specific dissipation rate (gray line), ω , at the inlet (continuous line) and at the incident building position (dashed line) in the empty domain. The subscripts in and ic refer to inlet and incident, respectively. The height of the model (h) is 0.123 m.

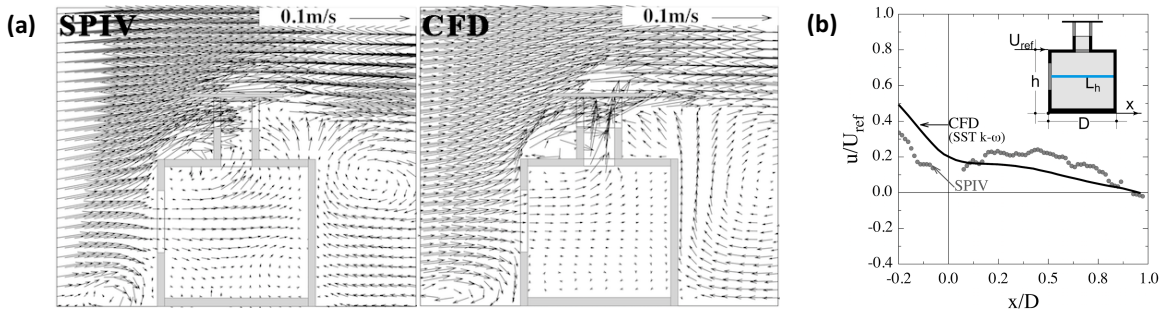


Figure 4. Experimental (SPIV) and numerical (CFD) results: (a) Velocity vector field at the central plane and (b) Streamwise speed ratio u/U_{ref} along the central line L_h .

Application example of HBI

To evaluate the thermal comfort produced by natural ventilation inside the building by using the HBI, the computational parameters and settings presented in Section CFD Validation are employed. Note that, the simulations done in that section reproduces the experimental conditions, in which the building is scaled 1/25. To obtain direct results in full scale, the domain and the building are rescaled to full scale by maintaining geometric similarity. For the application example, the numerical results are averaged over the last one hundred iterations to obtain a reliable steady numerical solution of an intrinsically unsteady flow phenomena performed with a RANS turbulence model. The U_{ref} is taken from the weather data for calculating the inlet velocity profile and it is used in the kinematic similarity calculations. The interior volume is discretized in 3375 cells of which the air velocity magnitude is obtained. Then, the HBI is calculated with the following data: Radiant temperature, T_r ; Ambient temperature, T_a ; Relative humidity, RH ; Reference air velocity, U_{ref} , and Metabolic heat production, M .

The HBI application example is performed with the averages of the maximum values of the hottest and most humid month (August) in the Temixco city located in Morelos, Mexico. These conditions are $U_{ref} = 3.5$ m/s (the reference air velocity at $h = 2.25$ m building height), $T_r = T_a = 27$ °C and $RH = 80\%$. The $U(z)$ from the real scale are modeled as inlet boundary condition, in the validated numerical model, by applying the dynamic similarity with $Re = U_{ref} h/\nu = 6.85 \times 10^5$. Fig. 5 shows the comfort evaluation by natural ventilation of the building

with a window and a windexchanger (Fig. 1), applying Eq. (5) and considering a metabolic heat production of $M = 93 \text{ W/m}^2 = 1.6 \text{ met}$ (light activity). The interior volume can be zoned as: discomfort by low ventilation (hot discomfort), D_{lv} , comfort, C , and discomfort by high ventilation (cold discomfort), D_{hv} . In this example, the percentages of D_{lv} , C , and D_{hv} zones are 65%, 30% and 5%, respectively, indicating that for these climatic conditions the cross ventilation in this specific building is not enough to provide thermal comfort in most of the building interior.

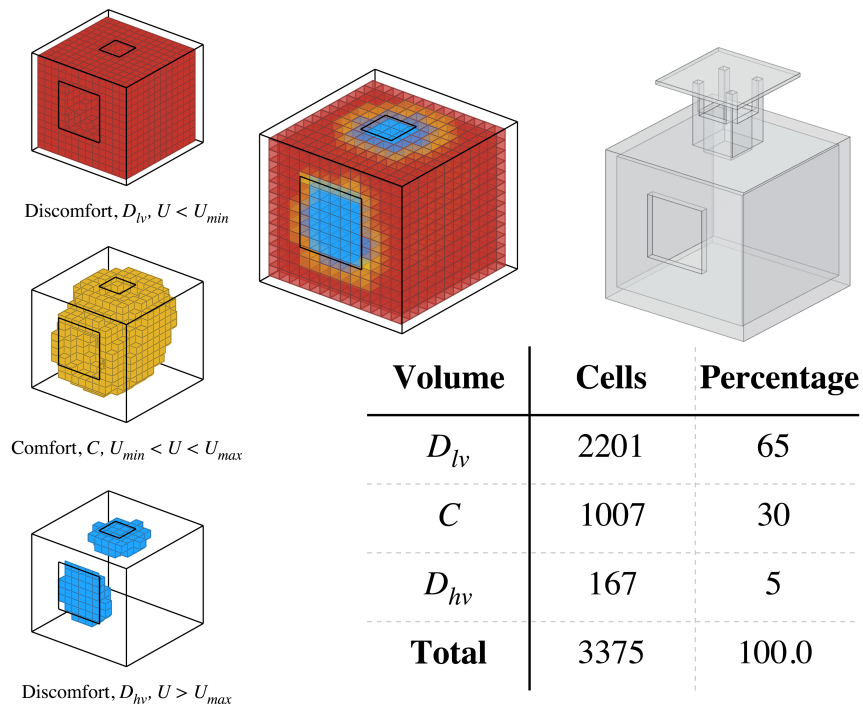


Figure 5. Evaluation of the comfort by natural ventilation of a building with cross ventilation. The interior volume is zoned as: discomfort by low ventilation, D_{lv} , comfort, C , and discomfort by high ventilation, D_{hv} . The range $U_{min} \leq U \leq U_{max}$ refers to the comfort air velocity range.

Discussion and conclusions

This paper provides an application example of this methodology using numerical simulations with CFD. The results of the application example only are valid for the described values of the building geometry, radiant temperature, ambient temperature, relative humidity, reference air velocity and metabolic heat production.

The HBI gives the comfort air velocity range, which is useful to calculate the well-ventilated percentage of an indoor space for a specific climate condition in hot climates and to assess the effect of a given strategy for natural ventilation. This can be done with CFD results or with experimental ones. Further research should be done to include the thermal adaptability in the HBI mathematical model.

Acknowledgements

This work has been supported by the PAPIIT-UNAM IN103816 project. The first author acknowledges the postdoctoral fellowship grant by the DGAPA-UNAM. The authors also thank to Dr. Maximiliano Valdez for the software configuration support.

References

- Aynsley, R. M. (1974). Effects of air flow on human comfort, *Build. Sci.*, 9, pp. 91-94.
- Bastide, A., Lauret, P., Garde, F., Boyer, H. (2006). Building energy efficiency and thermal comfort in tropical climates. presentation of a numerical approach for predicting the percentage of well-ventilated living spaces in buildings using natural ventilation. *Energy Buildings*, 38, pp. 1093-1103.
- Belding, H. S., Hatch, T. F. (1955). Index for evaluating heat stress in terms of resulting physiological strains. *Heating Piping and Air Conditioning*, 27, pp. 129-136.
- Blocken, B., Stathopoulos, T., Carmeliet, J. 2008. A numerical study on the existence of the Venturi- effect in passages between perpendicular buildings. *Journal of Engineering Mechanics ASCE* 12, 134, pp. 1021–1028.
- Castillo, J. A., Huelsz, G. (2017). A methodology to evaluate the indoor natural ventilation in hot climates: Heat Balance Index. *Building and Environment*, 114, pp. 366-373.
- Castillo, J. A., Huelsz, G., Cruz, M. V. (2014). Natural ventilation by windcatchers: CFD simulations and experiments. *CWE 2014, 6th International Symposium on Computational Wind Engineering*, Hamburg, Germany.
- COMSOL. 2013. *COMSOL module CFD user guide*. U.S.: COMSOL AB.
- Cruz-Salas, M.V., Castillo, J. A., Huelsz, G. (2014). Experimental study on natural ventilation of a room with a windward window and different windexchangers. *Energy and Buildings*, 84, pp. 458–465.
- De Dear, R. J., Brager, G.S. (2002). Thermal comfort in naturally ventilated buildings: revisions to ASHRAE standard 55, *Energy Buildings*, 34, pp. 549-561.
- Energy Efficiency Best Practice Programme (EEBPP) (1993). *Energy Consumption Guide 19. Energy Efficiency in Offices*, Energy Efficiency Office/HMSO.
- Etheridge, D. (2012). *Natural ventilation of buildings – Theory, measurement and design*. Chichester: John Wiley and Sons.
- Fanger, P. (1970). *Thermal Comfort Analysis and Applications in Environmental Engineering*. Engineers McGraw-Hill, New York.
- Givoni, B. (1969). *Man, Climate and Architecture*, Elsevier Architectural Science Series, Elsevier, Amsterdam - London - New York.
- Humphreys, M. A., Nicol, J.F. (1998). Outdoor temperature and indoor thermal comfort: raising the precision of the relationship for the 1998 ASHRAE database of field studies, *AHSRAE Trans*, 206, pp. 485-492.
- Liping, W. and Hien, W.N. (2007). The impacts of ventilation strategies and facade on indoor thermal environment for naturally ventilated residential buildings in Singapore. *Building Environment*, 42, pp. 4006-4015.
- Prianto, E., Depecker, P. (2002). Characteristic of airflow as the effect of balcony, opening design and internal division on indoor velocity: a case study of traditional dwelling in urban living quarter in tropical humid region. *Energy Buildings*, 34, pp. 401-409.
- Ramponi, R., Blocken, B. (2012). CFD simulation of cross-ventilation for a generic isolated building: Impact of computational parameters. *Building and Environment*, 53, pp. 34–48.
- Su, X., Zhang, X., Gao, J. (2009). Evaluation method of natural ventilation system based on thermal comfort in China. *Energy Buildings*, 41, pp. 67-70.
- Tominaga, Y., Mochida, A., Yoshie, R., Kataoka, H., Nozu, T., Yoshikawa, M. (2008). AIJ guidelines for practical applications of CFD to pedestrian wind environment around buildings. *Journal of Wind Engineering and Industrial Aerodynamics*, 96, pp. 1749–1761.
- Yang, L. (2003). *Climatic Analysis and Architectural Design Strategies for Bio-climatic Design*, Climatic Analysis and Architectural Design Strategies for Bio-climatic Design.
- Wang, L., Liu, J., Liu, Y., Wang, Y., Chen, J. (2011). Study on thermal environment of traditional architecture in tropic climate, *Advance Materials Research*, pp. 6857-6861.